

Stopping light in two dimensional quasicrystalline waveguides

A.Trabattoni,^{1,2*} L.Maini,¹ G. Benedek^{1,3}

¹ *Dipartimento di Scienza dei Materiali, Università Milano-Bicocca, Via R. Cozzi 53, 20125 Milano, Italy*

² *Dipartimento di Fisica, Politecnico di Milano, Piazza Leonardo da Vinci 32, 20133 Milano*

³ *Donostia International Physics Center (DIPC), Universidad del País Vasco (UPV/EHU), P. Manuel de Lardizàbal 4, 20018 Donostia / San Sebastián, Spain*

[*andrea1.trabattoni@mail.polimi.it](mailto:andrea1.trabattoni@mail.polimi.it)

Abstract: The introduction of defects in photonic lattices generally allows to control the localization and the propagation of light. While point defects are conventionally used in order to obtain localized photonic states, linear defects are introduced for waveguiding EM waves. In this work we demonstrate the possibility of obtaining localized states also in a waveguiding configuration, by using quasicrystalline lattices. This result opens a new range of possibilities in designing optical circuits, in which the localization-propagation switch is easily obtainable by mechanical or opto-electric methods.

© 2012 Optical Society of America

OCIS codes: (050.5298) Photonic crystals; (130.5296) Photonic crystal waveguides.

References and links

1. E. Yablonovitch, "Inhibited spontaneous emission in solid-state physics and electronics," *Phys. Rev. Lett.* **58**, 2059-2062 (1987)
2. S. John, "Strong localization of photons in certain disordered dielectric superlattices," *Phys. Rev. Lett.* **58**, 2486-2489 (1987)
3. E. Kuramochi, H. Taniyama, T. Tanabe, A. Shinya, and M. Notomi, "Ultrahigh-Q two-dimensional photonic crystal slab nanocavities in very thin barriers," *Applied Physics Letters* **93**, 111112 (2008)
4. E. Gavartin, R. Braive, I. Sagnes, O. Arcizet, A. Beveratos, T. J. Kippenberg, and I. Robert-Philip, "Optomechanical coupling in a two-dimensional photonic crystal defect cavity," *Phys. Rev. Lett.* **106**, 203902 (2011)
5. F. D. M. Haldane and S. Raghu, "Possible realization of directional optical waveguides in photonic crystals with broken time-reversal symmetry," *Phys. Rev. Lett.* **100**, 013904 (2008)
6. J. C. Knight, J. Broeng, T. A. Birks, and P. S. J. Russell, "Photonic band gap guidance in optical fibers," *Science* **282**, 5393 (1998)
7. D. Shechtman, I. Blech, D. Gratias, and J. W. Cahn, "Metallic phase with long-range orientational order and no translational symmetry," *Phys. Rev. Lett.* **53**, 1951-1953 (1984)
8. D. Levine and P. J. Steinhardt, "Quasicrystals: a new class of ordered structures," *Phys. Rev. Lett.* **53**, 2477-2480 (1984)
9. Y. S. Chan, C. T. Chan, and Z. Y. Liu, "Photonic band gaps in two dimensional photonic quasicrystals," *Phys. Rev. Lett.* **80**, 956-959 (1998)
10. S. G. Johnson and J. D. Joannopoulos, "Block-iterative frequency-domain methods for Maxwell's equations in a planewave basis," *Opt. Express* **8**, 3, 173-190 (2001)
11. A. F. Oskooi, D. Roundy, M. Ibanescu, P. Bermel, J. D. Joannopoulos, and S. G. Johnson, "MEEP: a flexible free-software package for electromagnetic simulations by the FDTD method," *Computer Physics Communications* **181**, 687-702 (2010)
12. M. Oxborrow and C. L. Henley, "Random square-triangle tilings: A model for twelvefold-symmetric quasicrystals," *Phys. Rev. B* **48**, 6966-6998 (1993)
13. J. D. Joannopoulos, S. G. Johnson, J. N. Winn, and R. D. Meade, *Molding the Flow of Light* (Princeton University Press, 2008)

14. S. R. Davis, S.D. Rommel, G. Farca, and M. H. Anderson, "A new electro-optic waveguide architecture and the unprecedented devices it enables," Proc. SPIE **6975**, 697503 (2008)
15. W. Ruan, G. Li, J. Zeng, L. S. Kanzina, H. Zheng, K. Zhao, L. Zheng, and A. Ding, "Origin of the giant electro-optic Kerr effect in La-doped 75PMN-25PT transparent ceramics," J. Appl. Phys. **110**, 074109 (2011)

1. Introduction

The vast research areas of optoelectronic and photonic devices have been given a substantial boost by Yablonovich and John's discovery of photonic crystals (PCs) [1, 2]. Among the most interesting applications of PCs there is the possibility of manipulating the group velocity of electromagnetic waves in dielectric materials. Considerable attention has been given to the role of defects in photonic lattices, in view of the fact that special defect configurations allow to control the propagation of light in various ways: point defects are conventionally used in order to obtain localized states [3, 4], whereas linear defects are introduced as waveguides [5, 6]. Linear defects in photonic lattices exploit a remarkable feature of PC, i.e. the ability to guide light in vacuum (air). Whereas conventional dielectric waveguides work through the mechanism of internal reflection, thus confining light in a region of high dielectric constant, PC waveguides exploit the presence of a photonic bandgap in the surrounding crystal which prevents light to escape. This ability is fundamental for many applications in which it is desirable to reduce the interactions, such as absorption or nonlinearity, between light and the dielectric materials. Two questions are addressed in this Letter: 1) whether a regular linear structure can be designed so as to allow for either localized (trapped) or guided free-propagating photon states; 2) whether a switch is possible from localized to propagating photon states with a controlled group velocity. These properties would allow to design new optical circuits in which localization, waveguide propagation and controlled group velocity of light are implemented in the same configuration. It is found that a photonic quasicrystal (PQC) [7–9] is suitable to the purpose: due to the combination of a high-order point symmetry at distinct points of the lattice with an orientational long-range order, localized modes may exist which are degenerate with freely propagating modes.

2. Results and Discussion

In this work a waveguide is designed out of a two-dimensional (2D) dodecagonal photonic quasicrystal, and thoroughly investigated by means of simulations with the MPB [10] and MEEP [11]. The quasicrystal geometry is constructed by a tiling method known as Stampfli inflation [12] (Fig.1(a)), with a constant distance a between nearest-neighbour lattice nodes and rods of radius $0.3a$, located at each lattice node. The photonic band structure for stationary electromagnetic modes in a PQC is obtained by solving the time-independent Maxwell equation for the magnetic field $\mathbf{H}(\mathbf{r})$

$$\nabla \times \left(\frac{1}{\varepsilon(\mathbf{r})} \nabla \times \mathbf{H}(\mathbf{r}) \right) = \left(\frac{\omega}{c} \right)^2 \mathbf{H}(\mathbf{r}), \quad (1)$$

where ω is the angular frequency, c the speed of light, and $\varepsilon(\mathbf{r})$ the position-dependent dielectric constant. The present PQC model is constituted by rods of alumina ($\varepsilon = 8.6$), a material largely used in photonic crystals, surrounded by vacuum ($\varepsilon = 1$), which allows for a sufficiently large contrast. In order to study the optical properties of this system through a simulation of the photonic band structure, a supercell approximant with periodic boundary conditions needs to be defined in order to restore, and take advantage from, periodicity on the large scale. We consider first a rectangular supercell containing 116 rods (Fig.1(b)) with periodic boundary conditions in both x and y directions and refer to this system as the bulk configuration. An important requirement in imposing the periodicity in the y direction is that adjacent unit cells are also connected

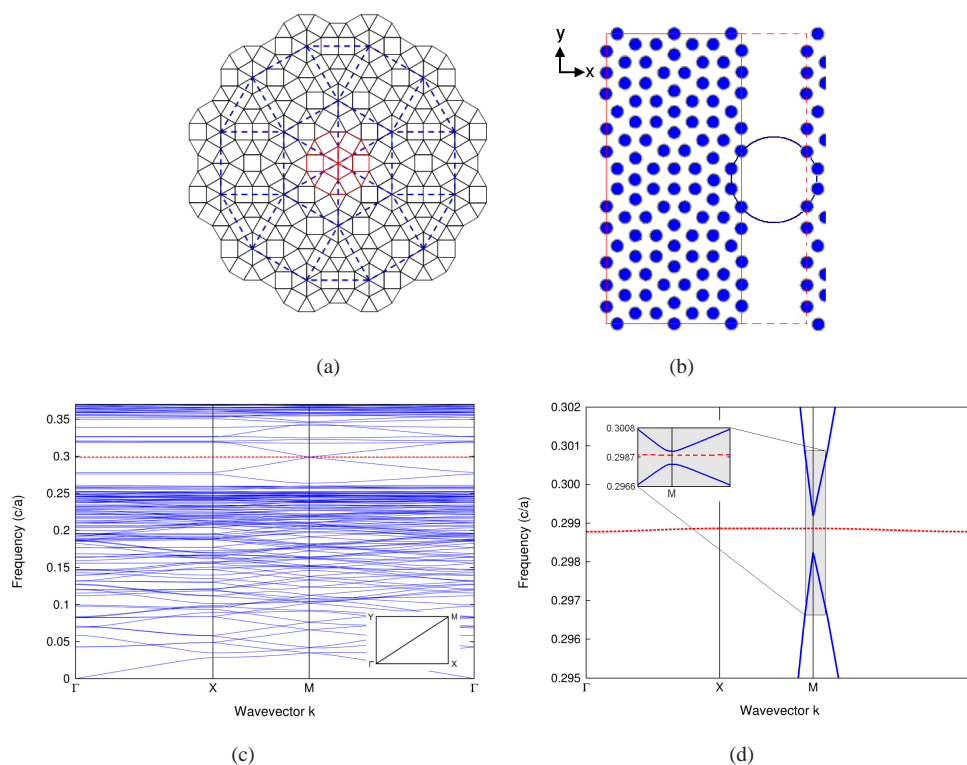


Fig. 1. (a) Illustration of the Stampfli inflation rule. (b) Dielectric distribution of the supercell approximant used in the calculations. The rectangular supercell for the calculation of the $2D$ bulk band structure (full line) contains 116 rods of alumina with $\epsilon = 8.6$ and radius $r = 0.3a$, surrounded by vacuum ($\epsilon_0 = 1$). Periodic boundary conditions in x and y directions are imposed, so as to take advantage of translational symmetry. With a 50% extension of the supercell in the x direction (broken line) a vacuum slab is inserted so as to create a periodic array of quasi-crystalline slabs separated by vacuum cavities. In this case small indentations (as the one evidenced by the circle) appear along the slab contours. (c) Photonic band structure of the dodecagonal photonic quasicrystal in slab configuration. An almost perfectly flat branch (red dashed line), corresponding to strongly localized states, occurs in the gap at a frequency (zone-center value) $\nu = 0.298779c/a$. In the inset the irreducible Brillouin zone is shown. (d) On a magnified scale the flat branch shows a little dispersion. At the M point the flat branch is localized in a small gap between two narrow tips of the dispersed branch (inset).

by the same squares and equilateral triangles characterizing Stampfli inflation (Fig. 1(b)), so as to ensure structural continuity and avoid mismatch defects. The photonic dispersion curves for the bulk and the magnetic field polarized in plane (TM polarization) show a large frequency band gap of about $0.1c/a$ between $\nu = 0.25c/a$ and $0.35c/a$, where c is the speed of light in vacuum. On the contrary the dispersion curves for the electric field polarized in the plane (TE-polarization) do not exhibit any complete band gap.

When a linear defect is inserted new localized states, known as defect modes, appear in the spectrum with dispersion curves which completely fill the band gap [13]. A similar situation can be obtained in the $2D$ periodic configuration illustrated in Fig.1(b) with an extension of

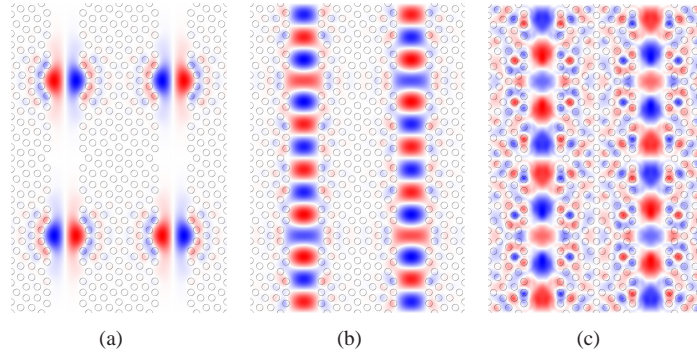


Fig. 2. (a) TM-polarized electric field distribution of the localized state at the Γ point. The field localization is the same all along the flat branch in the Brillouin zone. (b) A small perturbation in the dielectric constant produces a dispersion near the M point, and a consequent transformation of the electric field into a plane wave through the waveguide. The same result is obtained by slightly decreasing the vacuum region thickness. (c) On the contrary an increase of the vacuum region thickness cause a delocalization of the electric field into the slabs.

the supercell in the x direction (broken line) so as to create a periodic array of slabs separated by slab-shaped vacuum cavities. We shall refer to this system as the slab configuration. In this case a periodic sequence of indentations (Fig.1(b)) appears on each contour of the slab. Such indentations, suggesting small circular cavities, are peculiar of the dodecagonal symmetry and are seen below to host localized states. This actually occurs when the thickness of the vacuum region approaches the length of the indentations so as to make the cavity outlined by the two opposed indentations (Fig.1(b)) a perfect circle. The calculated TM band structure for this particular slab configuration is shown in Fig.1(c). An almost perfectly flat branch (red dashed line), corresponding to strongly localized states (Fig.2(a)), occurs in the gap at a frequency (zone-center value) $\nu = 0.298779 c/a$. Only in the ΓX direction of the Brillouin zone (the bottom of Fig.1(c)), where the flat branch intersects a folded dispersed branch, some weak dispersion appears together with a small gap between two narrow tips of the dispersed branch (Fig. 1(d) and inset). The very small dispersion of the flat branch can be expressed by the component v_x of the band group velocity, whose maximum value in the ΓX direction is $\simeq 3.05 \cdot 10^{-4} c$. Even smaller is the dispersion in the direction XM parallel to the slabs in the waveguide direction, which is only $\simeq 10^{-7} c$. It is interesting to note that the dispersion of the flat branch further decreases with the thickness of the slabs: for a double thickness the flat branch angular frequency at Γ is slightly shifted to $0.2988 c/a$ and the maximum group velocity along ΓX becomes also as small as $\simeq 10^{-7} c$. As expected, thicker slabs reduce the interaction between neighbour vacuum channels, thus leading to a stronger localization.

On the basis of this finding, two mechanisms of wave-guiding delocalization of the localized state have been investigated, which can be easily implemented in a double PQC slab configuration. The first mechanism is a perturbation of the dielectric constant. When the dielectric constant is suddenly decreased from 8.6 to 8.0 only in the rods adjacent to the vacuum region a little dispersion in the flat branch emerges near M point, in the y direction of the waveguide towards the exit into vacuum. The group velocity in XM direction is now increased to $v_y \simeq 5.8 \cdot 10^{-3} c$. The transition from a localized to a wave-guide propagation state is evident also in the corresponding electric field distribution: at the M point the state is now delocalized in the y direction along the waveguide, without dissipating energy into the slabs (Fig.2(b)). In

this way it is possible to transform the localized state into a waveguide mode with a small external perturbation. For a larger perturbation, e.g., $\epsilon = 7.0$ for the rods adjacent to the vacuum channel, the flat branch dispersion increases with its group velocity v_y , raising to $1.7 \cdot 10^{-2} c$. Note that the same transition from a localized to a propagating photonic state is obtained for a local increase of ϵ . The second mechanism to induce the transition from localized to prop-

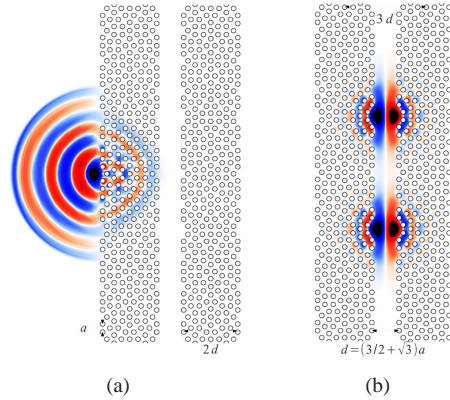


Fig. 3. (a) Z-component of the electric field after $10 a/c$, from a gaussian current source pulse $J(\omega, t) = (-i\omega)^{-1} \partial_t \exp(-i\omega t - (t - t_0)^2 / 2\sigma^2)$, centered at $\omega = 2\pi \cdot 0.298779 c/a$. The source has a frequency width of $1/\sigma = 0.005 c/a$ and it is turned off after $600 a/c$. (b) After $10^3 a/c$ the electro-magnetic radiation is almost completely trapped inside the cavity between the slab walls at the circular indentations, provided the vacuum region width is exactly $d = (3/2 + \sqrt{3})a$ (Media 1).

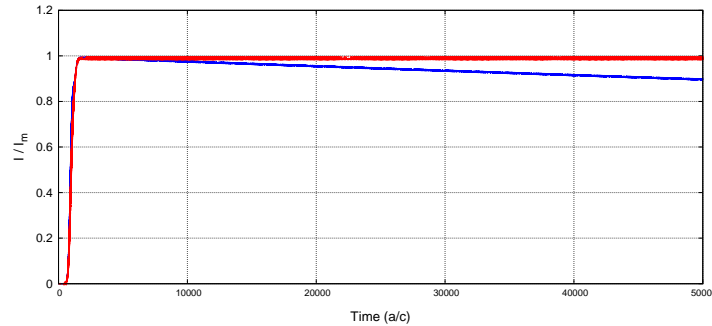


Fig. 4. The integral of the trapped EM energy, after reaching the maximum I_m (raise time of $\sim 10^3 a/c$), starts a very slow dissipation, linear with time. The dissipation time for the slab thickness of $2d$ is about $2 \cdot 10^{-6} I_m c/a$ (blue and thin line), but becomes much longer (red and tick line) for a doubled slab thickness of $4d$ and the same gap width.

agating waveguide states consists in a small increase of the vacuum region width, originally $d = (3/2 + \sqrt{3})a$. A change as small as $\Delta d = +0.05 a$ is sufficient to produce a delocalization of the state at the M point previously considered, but now much of field energy is spread into the slabs (Fig.2(c)). If the switch is inverted, e.g. the vacuum region width is decreased by the same amount ($\Delta d = -0.05 a$), the field distribution (as in Fig.2(b)) is completely different from the previous one: the guided-wave propagation occurs with no energy spread into the slabs, with a group velocity $v_y \cong 6.7 \cdot 10^{-3} c$. Again a perturbation twice as large ($\Delta d = -0.1 a$) yields the

same well guided wave propagation with a larger group velocity $v_y \simeq 1.7 \cdot 10^{-2} c$. This proves *the possibility of controlling the group velocity of a monochromatic electromagnetic wave inside a vacuum waveguide, and eventually stopping it in a localized state, by acting on the PQC with either an opto-electric or a mechanical perturbation.* It should be noted that even in systems with giant opto-electronic coefficients like liquid-crystal waveguides or doped ferroelectric perovskites refraction coefficient changes Δn hardly attain the percent range [14, 15]. However the present simulation with a local change of $\Delta n \simeq 1.5\%$ already transforms the localized mode into a plane wave travelling along the waveguide with a group velocity of $v_y \simeq 1.52 \cdot 10^{-3} c$.

The actual time-dependent behaviour of a single wave-guide made of two parallel PQC slabs of finite length (Fig.3), after an electromagnetic wave has been injected by an external monochromatic Gaussian flash, has been studied in a further numerical experiment with the MEEP code. The two PQC slab system is now excited by a quasi-monochromatic light source with a frequency centred on the gap localized frequency discussed above, with the aim of computing the level of localization in this wave-guiding configuration and studying its temporal evolution. As expected, the electric field tends to be localized in the waveguide between the two slabs at the circular indentations. As soon as the localized state levels off, it begins to pulsate inside the vacuum region, with a change of polarity at each period of oscillation and a very low energy loss. The effect is better seen in the animation (Fig. 3(b) (Media 1)). In order to evaluate the degree of localization inside the waveguide the EM field energy density has been integrated over a region around the cavity of width $3d$ and plotted as a function of time in Fig.4 (thin line). The integrated density exhibits a slow dissipation, linear with time at a rate of about $2 \cdot 10^{-6} I_m c/a$, where I_m is the maximum value of the EM field energy integral, reached after the raise time ($\simeq 10^3 a/c$). It means that for $a = 1 \mu m$ the half of I_m is lost after $\simeq 1 ns$. The dissipation rate, as expected, is found to be strongly dependent on the slab thickness. For the same vacuum gap width d but a doubled slab thickness ($4d$) the dissipation time becomes dramatically longer, the rate dropping down to about $10^{-18} I_m c/a$ (Fig.4, thick line). This indicates that under these conditions an almost perfect localization can be preserved over time scales of no less than 10^{17} time steps (a/c), which means for a micrometric system ($a = 1 \mu m$) decay times of several minutes, $I/I_m = 0.97$ after $10^2 s$.

3. Conclusions

The possibility of trapping photons for a comparatively long time and switching from the localized to a free-propagating state with a controlled speed suggests a use of these PQC configurations for photonic memories, and in general for a large variety of photonic circuits, where the switch from localization to waveguiding can be realized in the same device, by small mechanical or opto-electric switches. In this respect the occurrence of trapped states with a controllable rotating field polarization, either clock- or counterclockwise, allows in principle for a spin coordinate, with possible applications in photonic devices for various purposes, including quantum computing.

Acknowledgments

One of us (GB) acknowledges Ikerbasque for support (proyecto ABSIDES) and many useful discussions with Professors Xavier Aizpurua and Pedro M. Echenique (DIPC, Donostia / San Sebastian, Spain). Another of us (AT) acknowledges DIPC for support and inspiring suggestions by Professor Xavier Aizpurua (DIPC) and Professor Stefano Longhi (Department of Physics, Politecnico di Milano, Italy).